CHEMISTRY
A EUROPEAN JOURNAL

DOI: 10.1002/chem.201003738

Synthesis, Characterization, and the Photochromic, Luminescence, Metallogelation and Liquid-Crystalline Properties of Multifunctional Platinum(II) Bipyridine Complexes

Yongguang Li,[a] Anthony Yiu-Yan Tam,[b] Keith Man-Chung Wong,*[b] Wen Li,[a]
Lixin Wu,*[a] and Vivian Wing-Wah Yam*[a, b, c]

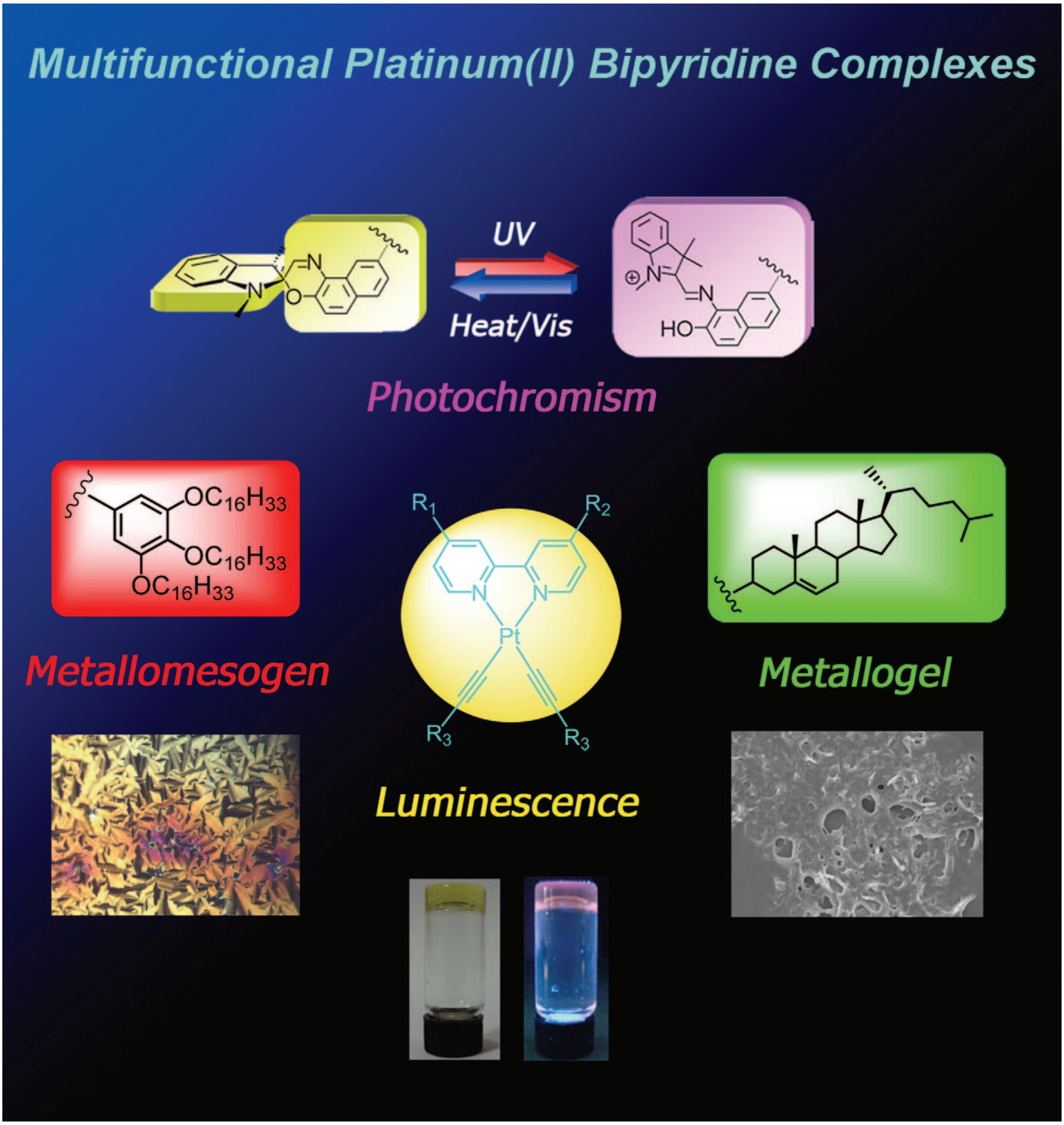

Abstract: A series of multifunctional platinum(II) bipyridine complexes were designed, synthesized, and characterized by ^{1}H NMR, fast atom bombardment mass spectrometry (FAB-MS), and elemental analysis. Their electrochemical and photophysical properties were investigated. The photochromic properties of the spironaphthoxazine-containing complexes were also studied. Some of these complexes were shown to be capable of forming stable thermoreversible metallogels in organic solvents. In contrast to typical thermotropic organogels and metallogels, one of the complexes could form metallogels in dodecane and is very stable towards external stimuli. The photochromic activation parameters for the bleaching reaction of a representative spironaphthoxazine-containing complex in a dodecane gel were determined through kinetic studies at various temperatures. Lamellar liquid-crystalline behavior was also observed in one of the complexes, and the liquid-crystalline properties were studied by thermogravimetry analysis (TGA), polarized optical microscopy (POM), differential scanning calorimetry (DSC), variable-temperature X-ray diffraction (XRD), and variable-temperature infrared (IR) spectroscopy.

Keywords: liquid crystals • luminescence • metallogels • photochromism • platinum • spironaphthoxazine

Introduction

Square-planar platinum(II) polypyridine complexes represent a unique class of transition-metal complexes due to their rich spectroscopic properties and propensity to form aggregate species through Pt···Pt and π-π stacking interactions in the solid and solution states.[1] Apart from the early works on the spectroscopic properties of dichloroplatinum(II) polypyridine complexes[1a,2] and their dicyano analogues,[1c,2b,3] the luminescent behavior of $[Pt(phen)(C\equiv CPh)_2]$ (phen = 1,10-phenanthroline, Ph = phenyl) has also been reported.[4] Since then, this class of square-planar platinum(II) complexes has received much attention due to their rich spectroscopic properties in both solid and solution states.[5] While there are extensive studies on the electrochemical, photophysical, and photochemical properties of this class of platinum(II) complexes, studies of their multifunctional properties are rare.[2d,e] Only quite recently have platinum(II) bipyridine complexes exhibiting photochromic[2d] and liquid-crystalline properties been reported.[2e]

Amongst various families that exhibit photochromic behavior, spirooxazines (SO) represent an interesting class of photochromic materials.[6] Owing to their high fatigue resistance and excellent photostability, their photochromic behavior has been extensively investigated for potential application in the development of materials such as sunglass lenses and optical recording since the 1980s.[6m,n] Similar to spiropyrans, the photochromic behavior of spirooxazines has been attributed to the photochemical cleavage of the spiro carbon–oxygen bond in SO forms that led to the planarization of the two originally orthogonal heterocycles to form merocyanine (MC) structures, giving rise to an increase in the extent of π-conjugation (Scheme 1). Much work has focused on organic systems, in which high-energy UV excitation is required for the intramolecular photosensitization of the photochromic spirooxazine moiety. It was only quite recently that examples of transition-metal complexes involving photosensitization of the photochromic behavior through excitation of lower-energy metal-to-ligand charge transfer (MLCT) bands in the visible region were reported.[6e,h,i,p–s]

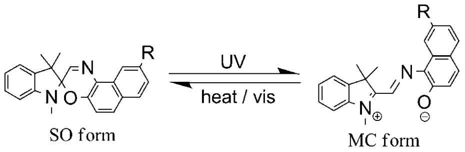

Scheme 1. Photoinduced ring-opening reaction of spironaphthoxazine.

In the past two decades, there has been an increasing interest in the study of new functional and stimuli-responsive low-molecular weight organogelators, because of their unique features and the increasing potential of the applications as soft matter in smart materials.[7–9] Early examples include the pioneering works of Weiss in anthracene- and anthraquinone-based gelators.[7a–c,f] It was found that the gelators could form stable organogels at low concentrations (ca. 1% by weight) solely through weak van der Waals interactions. Molecules exhibiting photochromic behavior have also been employed in the design of functional organogelators, including those of azobenzenes,[8a,10] diarylethenes,[11,12] spiropyrans,[13] and 2*H*-chromenes.[14] Recently, we reported a series of photochromic spironaphthoxazine-containing organogelators that is responsive to heat and acid.[15]

---

[a] Y. Li, Dr. W. Li, Prof. L. Wu, Prof. V. W.-W. Yam
State Key Laboratory of Supramolecular Structure and Materials
and College of Chemistry, Jilin University
Changchun 130012 (P.R. China)

[b] Dr. A. Y.-Y. Tam, Dr. K. M.-C. Wong, Prof. V. W.-W. Yam
Institute of Molecular Functional Materials and
Department of Chemistry, The University of Hong Kong
Pokfulam Road (Hong Kong)
E-mail: wwyam@hku.hk

[c] Prof. V. W.-W. Yam
Areas of Excellence Scheme
University Grants Committee (Hong Kong)

Parallel to the growing interest in the development of organogels, there has also been an immense interest in the investigation of transition-metal complexes as supramolecular gels,[16,17] for example, Au^I,[17a] Pt^{II},[17c,h,j,18] Cu^I,[17b] and Re^I complexes.[17i] Recently, alkynylplatinum(II) complexes with a terdentate N^N^N ligand were demonstrated to be capable of forming stable metallogels and were shown to display drastic color and emission changes during the gel-to-sol phase transition.[18a–c] These remarkable spectroscopic changes are believed to originate from the modulation of metal-to-metal-to-ligand charge transfer (MMLCT) transition resulting from aggregation-deaggregation processes of the square-planar platinum(II) complexes at different temperatures.

Besides the development of organogels and metallogels, liquid crystals have been investigated in supramolecular chemistry due to their huge potentials for application in a range of scientific and technological areas.[19] Phosphorescent metal complexes of Ag^I,[20] Au^I,[21] Pt^{II},[2e,22] and Pd^{II}[2e,22b,23] have been shown to exhibit diversified liquid-crystalline properties. Organometallic palladium(II) and platinum(II) with 2-phenylpyridine (C^N) ligands represent important classes of metallomesogens since rational modification of the structures would give rise to different phases of liquid crystals, including smectic phase, columnar mesophases, and nematic columnar mesophases.[22b,c]

Despite the development of photochromism, metallogelation and metallomesogens, studies of platinum(II) bipyridine complexes with multifunctional properties, such as photochromic[2d] and liquid-crystalline properties,[2e] are rare and often unexplored. Herein, we report the synthesis, electrochemistry, photophysical and photochemical properties of a series of multifunctional luminescent platinum(II) bipyridine complexes. Three of the complexes (**2**, **4**, and **10**) are found to exhibit stable thermotropic metallogels in organic solvents. The photochromic activation parameters for the bleaching reaction of the spironaphthoxazine-containing complex **10** in a dodecane gel were determined through kinetic studies at various temperatures. In addition, complex **2** was found to show liquid-crystalline behavior. Their properties were studied by thermogravimetric analysis (TGA), polarized optical microscopy (POM), differential scanning calorimetry (DSC), variable-temperature X-ray diffraction (XRD), and variable-temperature infrared (IR) spectroscopy.

Results and Discussion

Synthesis and characterization: Complexes **1** and **2** were synthesized according to a modification of a previously reported method for $[Pt(bpy)Cl_2]$[2] (bpy = 2,2′-bipyridine) using $[Pt(dmso)_2Cl_2]$ as the starting material. Due to the lack of solubilizing groups in **1**, it was found to be only fairly soluble in chloroform and dichloromethane. Complexes **3**–**10** were prepared by the reaction of the corresponding dichloroplatinum(II) bipyridine precursors and alkyne ligands in the presence of a catalytic amount of copper(I) iodide and diisopropylamine in dichloromethane. The identities of all the newly synthesized platinum(II) bipyridine complexes were confirmed by ^1H NMR spectroscopy, fast atom bombardment mass spectrometry (FAB-MS) and satisfactory elemental analyses.

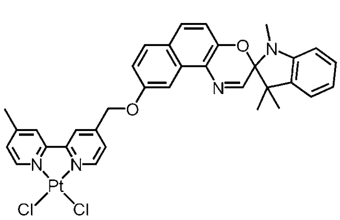

1

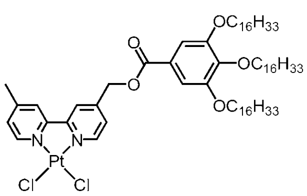

2

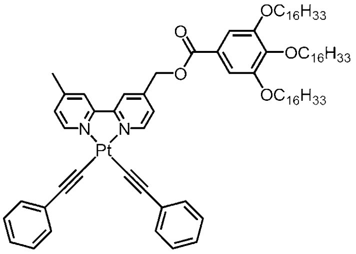

3

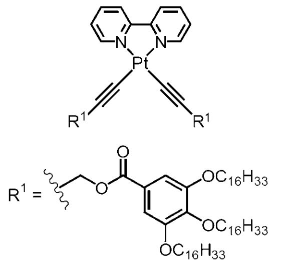

4

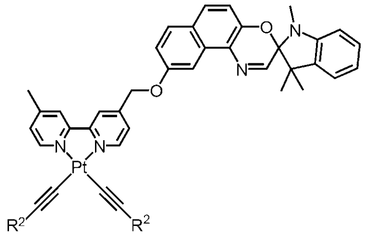

$R^2 = C_6H_5$ **5**

$R^2 = C_6H_4\text{–}(OCH_3)\text{–}4$ **6**

$R^2 = C_6H_4\text{–}(CF_3)\text{–}4$ **7**

$R^2 = C_6H_2\text{–}(OC_{12}H_{25})\text{–}3,4,5$ **8**

$R^2 = C_6H_2\text{–}(OC_{16}H_{33})\text{–}3,4,5$ **9**

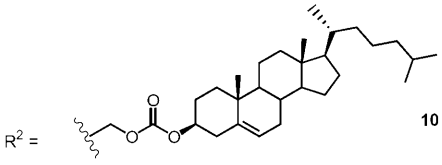

10

Electrochemistry: In general, the cyclic voltammograms of the platinum(II) bipyridine complexes in dichloromethane in the presence of nBu_4NPF_6 (0.1 M) displayed one quasi-reversible reduction couple at about −1.29 to −1.39 V and an irreversible anodic wave at approximately +0.80 to +1.30 V versus SCE. The electrochemical data of all of the complexes are summarized in Table 1. According to previous electrochemical studies on platinum(II) bipyridine complexes,[5a,b] the quasi-reversible reduction couples originate from the reduction of the bipyridine ligand. Apart from the quasi-reversible reduction couples, additional irreversible reduction waves were also observed at −0.90 to −1.27 V versus SCE in complexes **2**–**4**, which contain ester groups. In view of the observation of a similar irreversible reduction

Table 1. Photophysical and electrochemical data of platinum(II) bipyridine complexes.

	Medium	Absorption	Emission		Oxidation	Reduction
	(T [K])	λ_{max} [nm] (ε_{max} [dm^{3}mol^{-1}cm^{-1}])	λ_{em} [nm] (τ_o [μs])	ϕ_{em}[a]	E_{pa} [V] vs. SCE[b,c]	E [V] vs. SCE[b]
1	CH_2Cl_2 (298)	281 (41 910), 310 (17 285), 324 (18 410), 393 (5555)	572[d]	–[e]	–[f]	−1.35[g]
	solid (298)		–[i]	–		
	solid (77)		–[i]			
	glass[j] (77)		–[i]			
2	CH_2Cl_2 (298)	283 (29 910), 309 sh (7965), 322 (5425), 394 (2900)	550[d]	–[e]	–[f]	−1.22,[h] −1.30[g]
	solid (298)		–[i]			
	solid (77)		–[i]			
	glass[j] (77)		–[i]			
3	CH_2Cl_2 (298)	285 (56 870), 402 (7850)	570 (0.72)	0.2	0.98[k]	−1.29,[h] −1.38,[g]
	solid (298)		650			
	solid (77)		646			
	glass[j] (77)		518			
4	CH_2Cl_2 (298)	275 (31 635), 309 sh (12 330), 322 (8520), 371 (3460)	519 (0.61)	6.7×10^{-3}	0.85[k]	−0.95,[h] −1.30[g]
	solid (298)		618			
	solid (77)		620			
	glass[j] (77)		502			
5	CH_2Cl_2 (298)	286 (59 140), 400 (9095)	582 (0.32)	4.0×10^{-3}	1.04[k]	−1.33[g]
	solid (298)		–[i]			
	solid (77)		–[i]			
	glass[j] (77)		–[i]			
6	CH_2Cl_2 (298)	280 (44 520), 346 sh (10 175), 397 (5300), 442 sh (3,410)	619 (4×10^{-3})	3.0×10^{-3}	0.92[k]	−1.29[g]
	solid (298)		–[i]			
	solid (77)		–[i]			
	glass[j] (77)		–[i]			
7	CH_2Cl_2 (298)	291 (50 165), 347 sh (8790), 391 (7540)	551 (0.78)	2.3×10^{-3}	1.13[k]	−1.30
	solid (298)		–[i]			
	solid (77)		–[i]			
	glass[j] (77)		–[i]			
8	CH_2Cl_2 (298)	289 (70 630), 348 sh (13 025), 403 (8710)	612 (2.3×10^{-3})	9.4×10^{-2}		
	solid (298)		682			
	solid (77)		584			
	glass[j] (77)		583			
9	CH_2Cl_2 (298)	289 (63 965), 345 sh (13 540), 403 (8805)	605 (1.5×10^{-3})	9.4×10^{-2}	1.03[k]	−1.33
	solid (298)		672			
	solid (77)		592			
	glass[j] (77)		589			
10	CH_2Cl_2 (298)	287 (36 705), 310 sh (18 900), 322 (18 723), 347 sh (12 125), 398 sh (6910)	609 (7.8×10^{-3})	1.2×10^{-3}	1.22[k]	−1.39
	solid (298)		660			
	solid (77)		656			
	glass[j] (77)		–[i]			

[a] The luminescence quantum yield, measured at room temperature using $[Ru(bpy)_3]Cl_2$ as a standard. [b] In a dichloromethane solution with 0.1 M $n\mathrm{Bu_4NPF_6}$ (TBAH) as the supporting electrolyte at room temperature; scan rate 200 mV s^{-1}. [c] E_{pa} refers to the anodic peak potential for the irreversible oxidation waves. [d] The emission was too weak to be measured. [e] The luminescence quantum yield was not obtained because the emission was too weak to be measured with certainty. [f] An oxidation wave was not observed within the solvent window. [g] Quasi-reversible reduction wave; $E_{1/2} = (E_{pa}+E_{pc})/2$; E_{pa} and E_{pc} are the anodic peak and cathodic peak potentials. [h] Irreversible reduction wave. [i] Nonemissive. [j] In ethanol/methanol/dichloromethane = 4:1:1. [k] Irreversible oxidation wave.

wave at −1.08 V versus SCE for the free bipyridine ligand with an ester group in addition to the quasi-reversible bipyridine reduction couple at −1.38 V versus SCE, the irreversible reduction wave is tentatively assigned to the reduction of the ester group on the bipyridine or alkynyl ligands.[24]

Owing to the sensitivity of the potential of the oxidation waves towards the electronic effect of the alkynyl ligands, the irreversible oxidation is attributed to the oxidation of Pt^{II} to Pt^{III}, with substantial mixing of the alkynyl ligand characters. This assignment was further supported by the observation that the ease of oxidation increases in the order of **7** (+1.13 V) < **5** (+1.04 V) < **6** (+0.92 V), which is in line with the order of the electron-donating ability of the alkynyl ligands, $C{\equiv}CC_6H_4OMe$-*p* (**6**) > $C{\equiv}CPh$ (**5**) > $C{\equiv}CC_6H_4CF_3$-*p* (**7**).

Photophysical properties: The electronic absorption spectra of complexes **1**–**10** in dichloromethane at 298 K showed intense absorption bands at 275–348 nm and moderately intense absorption bands at 371–442 nm. The photophysical data of **1**–**10** are summarized in Table 1 and the electronic absorption spectra of complexes **5**–**8** and **10** are shown in Figure 1 (top). With reference to previous studies on platinum(II) bipyridine complexes[5] and related spironaphthoxazine-containing transition-metal complexes,[6e,h,j] the high-energy intense absorption bands are assigned to the intrali-

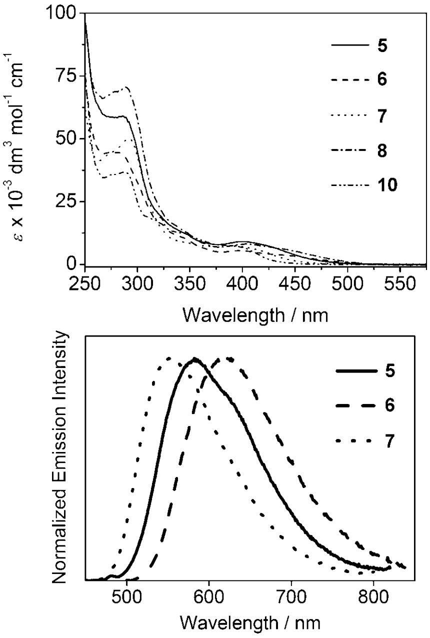

Figure 1. Top: UV/Vis absorption spectra of complexes **5**–**8** and **10** in a solution of dichloromethane at room temperature. Bottom: Normalized emission spectra of complexes **5**–**7** in degassed dichloromethane at 298 K.

gand (IL) [$\pi\rightarrow\pi^*$] transitions of the indoline, bipyridine, naphthoxazine moieties and alkynyl ligands, whereas the low-energy, moderately intense absorption bands are tentatively assigned as an admixture of metal-to-ligand charge transfer (MLCT) [$d\pi(Pt)\rightarrow\pi^*(bpy)$] and ligand-to-ligand charge transfer (LLCT) [$\pi(C\equiv C)\rightarrow\pi^*(bpy)$] transitions. The MLCT/LLCT assignment was further supported by the observation that the low-energy absorption bands showed an energy trend of **7** (391 nm) > **5** (400 nm) > **6** (442 nm), since the electron-donating methoxy substituent on the arylalkynyl ligand in complex **6** would raise the $d\pi(Pt)$ and $\pi(C\equiv C)$ orbitals in energy, which would result in a lowering of the MLCT/LLCT energy.[15a,b,18b] Complexes **8** and **9** showed essentially identical UV/Vis absorption patterns with similar molar extinction coefficients, suggesting that the chain length of the alkoxy groups on the arylalkynyl ligand has no significant effect on the MLCT absorption.

Upon excitation at $\lambda \geq 400$ nm, all of the complexes except **1**, **2**, and **5**–**7** showed luminescence properties in solution, the solid state, and the glass state. In dichloromethane at room temperature, all of the complexes showed a broad emission band at about 519–619 nm. The emission spectra of **5**–**7** are shown in Figure 1 (bottom). The emission energies of the complexes were found to be sensitive to the nature of the substituents on the arylalkynyl ligand. Complex **6**, which contains an electron-donating methoxy substituent on the arylalkynyl ligand, showed the lowest emission energy, while complex **7** with most electron-poor trifluoromethyl substituent showed the highest emission energy. This trend is consistent with an assignment of triplet ^{3}MLCT excited state mixed with triplet ^{3}LLCT character (^{3}MLCT/^{3}LLCT). It is worth noting that upon introduction of phenylalkynyl ligands to complex **2** to yield complex **3**, the emission was found to be enhanced with the observation of a redshift in energy. It is believed that the substitution of weak-field chloro ligands by strong σ-donating phenylalkynyl ligands would lead to a larger d-d orbital splitting and thereby raises the energy of the non-emissive ligand field excited state. As a result, the ^{3}MLCT/^{3}LLCT emission was enhanced. It is interesting to note that the photoluminescence quantum yield of **3** ($\phi_{em}=0.2$) is much higher than that of **5** ($\phi_{em}=0.004$). The substantial decrease in the photoluminescence quantum yield from **3** to **5** is attributed to an efficient intramolecular energy transfer from the emissive ^{3}MLCT excited state to the spironaphthoxazine moiety for the photochromic process, rendering the photoluminescence from the ^{3}MLCT excited state less efficient.[6h,r] However, one should be aware that the assignments of electronic transitions between metal and/or ligand localized orbitals and singlet and triplet states are only rough approximations because of the possible extensive orbital mixing and spin-orbit coupling in these complexes.

Photochromic properties: On prolonged irradiation at $\lambda =$ 350 nm, complexes **1** and **5**–**10** in dichloromethane changed color from yellow to blue. This was attributed to a photochromic reaction, in which the relatively weak spiro carbon–oxygen bond is photocleaved, resulting in the formation of the MC complex (Scheme 1). Interestingly, prolonged excitation into the absorption band of the admixture of singlet MLCT and singlet LLCT (^{1}MLCT/^{1}LLCT) transition at $\lambda =$ 405 nm also leads to similar photochromic reactions. This could possibly be ascribed to the fact that the ^{1}MLCT/^{1}LLCT excited state would undergo facile intersystem crossing into the ^{3}MLCT/^{3}LLCT state, because of the heavy-metal effect exerted by the platinum(II) center, causing an intramolecular photosensitization reaction of the spironaphthoxazine.[6e] On prolonged excitation at $\lambda = 405$ nm in dichloromethane, a new absorption band at 600 nm appeared. The lower absorption energy of the MC form relative to the SO form is ascribed to the planarization of the molecule in the MC form, resulting in an increase in the extent of π conjugation throughout the spironaphthoxazine moiety.

Gelation properties: All of the complexes were tested for gelation properties in various organic solvents. It was found that **2** and **4** could form metallogels in decalin (a mixture of *trans* and *cis* isomers) at 10 °C with their respective critical gelation concentrations (c.g.c.) of 1.2×10^{-2} M and 3.1×10^{-2} M, and complex **10** with cholesteryl moieties could form stable gels in aliphatic solvents like heptane, octane, decane, as well as dodecane at room temperature. It is interesting to note that the metallogel of **10** in dodecane (2.4×10^{-3} M) was found to be stable even at 117 °C, which is close to the decomposition temperature of complex **10**. Also, the metallogel of **10** in dodecane was not influenced even after ultrasonication for about 10 min. This may possibly be attributed to strong interactions between the gelator molecules, resulting in a tight entrapment of the solvent molecules inside the gel network even at high temperatures. Since only complex **10** showed stable metallogelation behavior at room temperature, detailed characterization of the metallogel was only carried out for **10** in dodecane, and the metallogel of **10** in dodecane under visible light and under UV illumination are shown in Figures 2a and b, respectively. Upon prolonged irradiation at $\lambda = 405$ nm at 15 °C, the yellow gel turned blue (Figure 2c).

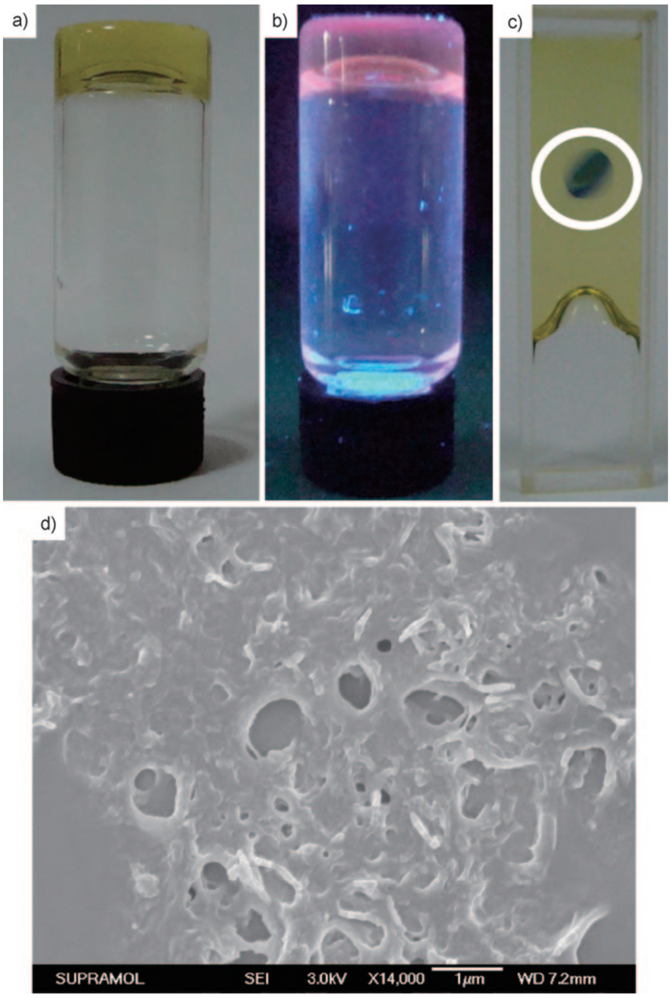

Figure 2. Photographs of the gel form of **10** (3.2×10^{-3} M) in dodecane a) under visible light and b) under 365 nm irradiation. c) Optical image of the dodecane gel of **10** at 15 °C showing the color change from yellow to blue upon prolonged excitation (indicated by circle). d) SEM image of the xerogel of **10** prepared from the dodecane gel of **10**.

The morphology of the dodecane gel of complex **10** was studied by scanning electron microscopy (SEM), and the SEM image of the xerogel is shown in Figure 2d. The xerogel showed a network of fibrous structures upon self-assembly in the gel phase. The fibers underwent further cross-linking to form three-dimensional fibrous networks to entrap the solvent molecules.

While no significant spectral change was observed in the variable-temperature electronic absorption study of the metallogel of **10** in dodecane, the corresponding emission study at variable temperatures showed a slight blueshift in the emission energy upon increasing the temperature (Figure 3, top left). This could possibly be attributed to the influence of the chromophoric interaction on going from the gel form to the sol form at elevated temperatures.

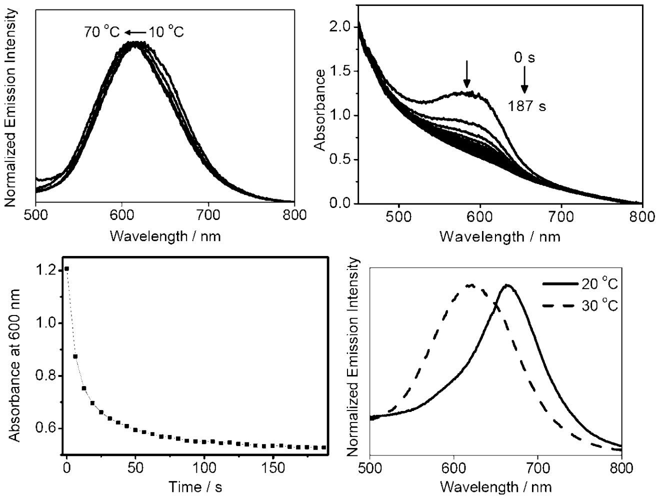

Figure 3. Top left: Normalized emission spectra of the dodecane gel of **10** upon increasing the temperature from 10 °C to 70 °C. Top right: Time-dependent UV/Vis absorption spectra of the dodecane gel of **10** (3.6×10^{-3} mol dm^{-3}) at 15 °C upon excitation at 405 nm. Bottom left: The absorption at 600 nm versus time. Bottom right: Normalized emission spectra of the dodecane gel of **10** upon prolonged irradiation at 405 nm at 20 and 30 °C.

Upon prolonged excitation into the ^{1}MLCT/^{1}LLCT absorption band ($\lambda = 405$ nm) at 15 °C, the dodecane gel of complex **10** changed from yellow to blue (Figure 2c) with the growth of a new absorption band at about 600 nm (Figure 3, top right). Similar to the results observed in dichloromethane, this was attributed to the photochromic reaction of the spironaphthoxazine moiety, which was sensitized by the ^{3}MLCT/^{3}LLCT excited state.[6e] The MC form generated was found to be thermally unstable and underwent rapid thermal bleaching to the SO form (vide infra), as indicated by the disappearance of the 600 nm absorption band after light irradiation even at 15 °C (Figure 3, bottom left) In addition, the prolonged excitation would also influence the emission energy. In the dark, the metallogel of **10** in dodecane showed an emission band at 620 nm at 20 °C, which is tentatively assigned as originating from the ^{3}MLCT of the SO form, with some mixing from the ^{3}LLCT state. Upon prolonged excitation into the ^{1}MLCT/^{1}LLCT absorption band, a new emission band at 664 nm was observed with diminishment of the 620 nm emission band at 20 °C. Upon increasing the temperature from 20 °C to 30 °C, the 664 nm emission disappeared with the revival of the emission at 620 nm (Figure 3, bottom right). At first glance, the

664 nm band was thought to be due to the emission of the MC form. Closer scrutiny indicated a rather unusual unsymmetrical band shape, suggesting that such a redshift in the emission energy upon irradiation may be a result of self-absorption effects arising from the growth of the MC absorption upon irradiation, because there is a significant overlap between the absorption of the MC form and the ^{3}MLCT/^{3}LLCT emission. This was further supported by the observation that a concentrated solution of **10** in dichloromethane showed similar redshifts in emission energy upon irradiation, which became less obvious upon dilution. In addition, the revival of the ^{3}MLCT/^{3}LLCT emission at 620 nm upon increasing the temperature to 30 °C could be attributed to the thermal bleaching reaction of the photomerocyanine form to afford the thermally stable SO form, in which self-absorption effects became negligible.

The kinetics for the bleaching reaction of the photochromic process of complex **10** in a dodecane gel after excitation at 405 nm were studied by UV/Vis absorption spectroscopy at various temperatures. The thermal backward reaction resulted in the fading of the blue color and a decay of the low-energy absorption band (Figure 3, top right). By monitoring the absorbance at 600 nm (Figure 3, bottom left), the kinetics for the bleaching reactions were measured and the activation parameters were determined using the Eyring and Arrhenius equations. The Eyring and Arrhenius plots are shown in Figure 4 and the activation parameters were determined. An activation energy (E_a) of 35.86 kJ mol^{-1}, activation enthalpy ($\Delta H^{\neq}$) of 32.85 kJ mol^{-1}, and activation entropy ($\Delta S^{\neq}$) of -158.60 J mol^{-1} K^{-1} were obtained for the bleaching reaction of the metallogel of **10** in dodecane.

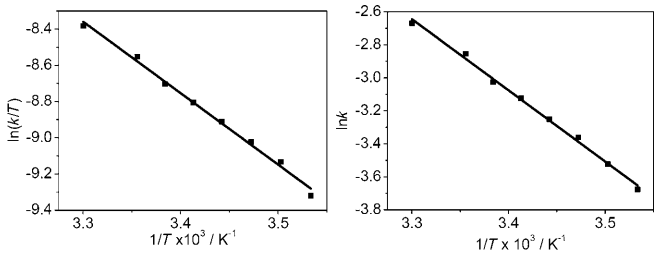

Figure 4. Eyring (left) and Arrhenius plots (right) for the thermal bleaching reaction of the dodecane gel of **10**.

Liquid-crystalline behavior: Since only complex **2** showed liquid-crystalline properties (Figure 5), it was subjected to the thermogravimetric analysis (TGA), polarized optical microscopy (POM), differential scanning calorimetry (DSC), variable-temperature X-ray diffraction (XRD) as well as variable-temperature infrared (IR) spectroscopy. Based on the TGA curve of complex **2** in the solid state (Figure 6, top left), it was found to be thermally stable up to a temperature close to 200 °C. The POM study showed that complex **2** exhibited two types of mesomorphic phases at 50 °C and 170 °C upon cooling from the isotropic state, as shown in

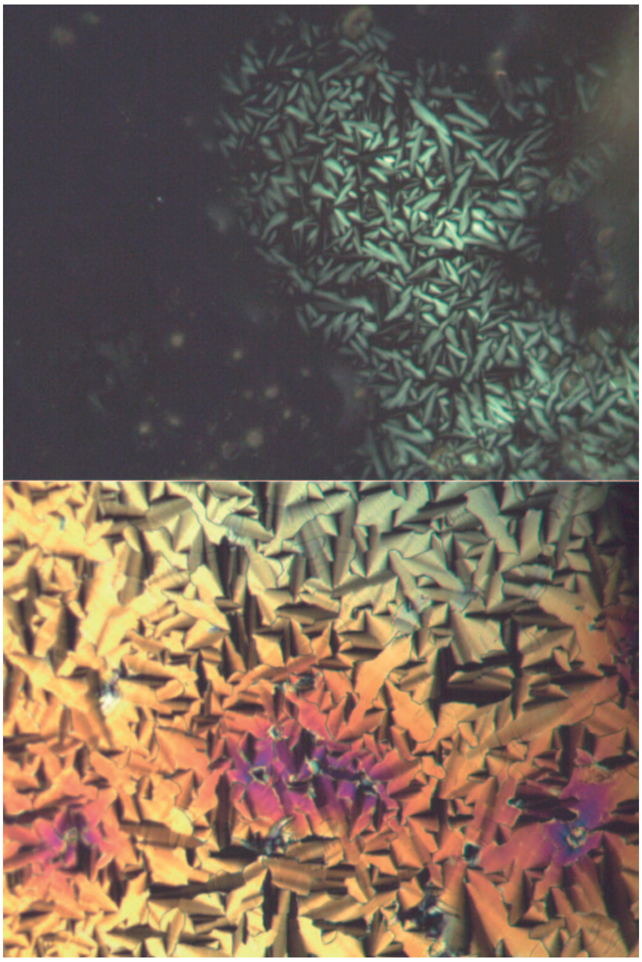

Figure 5. Polarized optical micrograph (×200 magnification) observed for complex **2** at 170 (top) and at 50 °C (bottom).

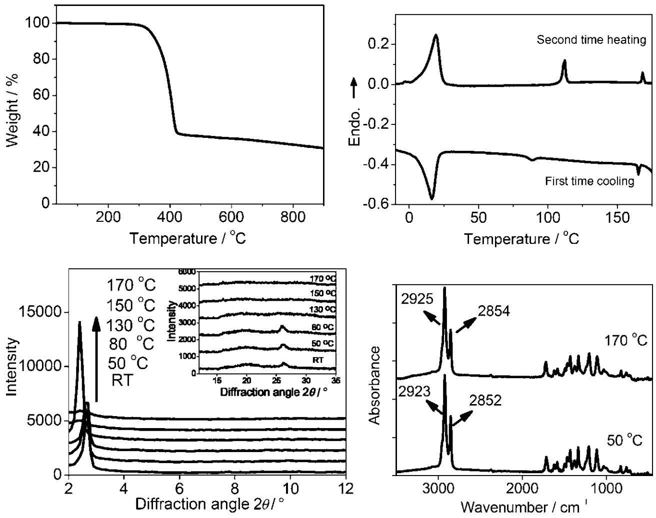

Figure 6. TGA thermograms (top left) and DSC heating and cooling curves (top right) of **2**. Bottom left: Variable-temperature XRD patterns of **2** in the temperature range from room temperature to 170 °C. Inset shows the magnified XRD patterns at high-angle regions. Bottom right: IR spectra of **2** at 50 °C and 170 °C.

Figure 5. The formation of these two phases was further confirmed by DSC studies that revealed the presence of two phase transitions in addition to the transformation into the isotropic phase (Figure 6, top right). The data are summarized in Table 2. The enthalpy change from the isotropic state to the first mesomorphic phase during the cooling process ($\Delta H = 1.38\ \text{kJ mol}^{-1}$) was relatively low, which suggested that the first mesomorphic phase was poorly ordered and a lamellar phase with two-dimensional positional order might probably be formed.

Table 2. Optical and thermal data for **2**.

Transition[a]	T [°C]	ΔH [kJ mol^{-1}]
C→SmC	19.3	34.26
SmC→SmA	111.9	4.85
SmA→I	168.6	1.32
I→SmA	165.6	−1.38
SmA→SmC	89.2	−1.40
SmC→C	16.4	−33.06

[a] C = crystal; SmA = smectic-A; SmC = smectic-C; I = isotropic liquid.

In order to investigate the molecular packing structure of the liquid crystal phase, variable-temperature XRD experiments were performed. Upon cooling from the isotropic state, a growth of elongated germs, so-called smectic *bâtonnets*, was observed at 170 °C. A commonly observed smectic-C (SmC) appeared at lower temperatures, as revealed by the broken texture (Figure 5, bottom), which resulted from the cooling of the smectic-A (SmA) to give SmC.[25b,d] According to the XRD pattern (Figure 6, bottom left), the very intense peak at the low-angle diffraction of $2\theta = 2.4°$, corresponding to the layer spacing,[25] and the diffuse halo at $2\theta \approx 20°$ are associated with the liquid-like two-dimensional organization of the mesogenic groups within the layer, suggestive of the formation of the SmA phase. The XRD data at 170 °C displayed one peak at 2.4° (2θ, corresponding to a d spacing of 37 Å) in the higher angle region of the XRD pattern, which lies between the length of a single molecule of **2** ($l = 32$ Å) and the length of two independent molecules ($2l = 64$ Å). It is known that the director $\boldsymbol{n}$ in the SmA phase and the optical axis are perpendicular to the smectic layer plane. It can be suggested that a double layer is organized in an intertwined fashion of the alkyl chains ($2l/d = 1.7$). Two broad peaks were also observed at the higher-angle region of the XRD pattern (d spacing = 4.5 and 3.5 Å) at lower temperatures, which could be attributed to the alkyl chain halo and the π-stacking distance, respectively. Upon increasing the temperature, the peak at low angle was shifted from 2.7 to 2.4° with diminishment of the intensity, and the broad peaks in the high-angle region were found to gradually disappear. These suggest that the order of the alkyl chains increased and the hydrophobic–hydrophobic interactions between the long chains and the π-stacking interactions became stronger at lower temperatures. This observation could be readily rationalized by the fact that upon increasing the temperature, the alkyl chains would undergo rapid vigorous motion and the intercalations would become less significant. As a result, the hydrophobic-hydrophobic and the π-stacking interactions would become less significant.

Variable-temperature IR spectroscopy was also employed to investigate the molecular packing of the liquid crystal phase. The IR data for the second heating cycle are shown in Figure 6 (bottom right). The stretching frequencies of the CH_2 antisymmetric and symmetric bands showed small shifts from 2923 and 2852 cm^{-1} at 50 °C to 2925 and 2854 cm^{-1} at 170 °C, respectively. It is known that the frequencies of the CH_2 antisymmetric and symmetric stretches are sensitive to the conformation of the alkyl chains. Low wavenumbers (2915–2920 and 2846–2850 cm^{-1}) are characteristic of a highly *trans* conformation of the alkyl chains, whereas their shifts to higher frequencies (2924–2928 and 2854–2856 cm^{-1}) are indicative of an increase in *gauche* conformers and an increase in the disorder of the alkyl chain conformation. Therefore, it is believed that the long chain has no significant influence on the packing of the molecules. This result suggested that the actual molecular length is smaller than that obtained by calculation ($l = 32$ Å).

Conclusion

In summary, a series of multifunctional photochromic spironaphthoxazine-containing platinum(II) bipyridine complexes was designed, synthesized and characterized. Their electrochemical, photophysical, photochromic, gelation and liquid-crystalline properties were investigated. Complexes **2**, **4**, and **10** were shown to be capable of forming stable thermoreversible metallogels in organic solvents. The activation parameters for the bleaching reaction of the complex **10** in a dodecane gel were determined by kinetic studies at various temperatures. Complex **2** was shown to display lamellar liquid-crystalline behavior, which was characterized by TGA, DSC, variable-temperature XRD, and variable-temperature IR studies.

Experimental Section

Materials and reagents: 4-(1,3,3-Trimethylspiroindolinenaphthoxazine-9′-oxymethyl)-4′-methyl-2,2′-bipyridine,[6h,j] 3,4,5-tri(dodecyloxy)phenylacetylene, 3,4,5-tri(hexadecyloxy)-acetylene,[18c] and Pt(bpy)Cl_2[2] were synthesized as described previously.

Syntheses

Synthesis of (4′-methyl-2,2′-bipyridin-4-yl)methyl-3,4,5-tris(hexadecyloxy)-benzoate: 4-(Bromomethyl)-4′-methyl-2,2′-bipyridine (222 mg, 0.84 mmol) was added to a mixture of 3,4,5-tris(hexadecyloxy)benzoic acid (600 mg, 0.72 mmol) and K_2CO_3 (165 mg, 1.2 mmol) in DMF (70 mL), under a nitrogen atmosphere. The reaction mixture was heated to reflux overnight. The reaction mixture was poured into deionized water, and a white precipitate appeared. After filtration, the white precipitate was washed with water (100 mL) and then methanol (100 mL) to yield the pure product. Yield: 302 mg, 41 %. ^{1}H NMR (500 MHz, $CDCl_3$, 298 K, relative to Me_4Si): $\delta = 0.88$ (t, $J = 6.8$ Hz, 9H; CH_3), 1.26–1.30 (m, 72H; CH_2), 1.45–1.46 (m, 6H; CH_2), 1.72–1.81 (m, 6H; CH_2), 2.45 (s, 3H; CH_3 on bpy), 3.97–4.01 (m, 6H; OCH_2), 5.43 (s, 2H; OCH_2 on bpy), 7.15 (d, $J = 5.3$ Hz, bipyridine proton at 5′-position), 7.32 (s, 2H; C_6H_2), 7.35 (d, $J=5.0$ Hz, bipyridine proton at 5-position), 8.25 (s, bipyridine proton at 3′-position), 8.46 (s, bipyridine proton at 3-position), 8.53 (d, $J=5.3$ Hz, bipyridine proton at 6′-position), 8.68 ppm (d, $J=5.0$ Hz, bipyridine proton at 6-position).

Synthesis of prop-2-ynyl-3,4,5-tris(hexadecyloxy)benzoate: Propargyl bromide (476 mg, 4 mmol) was added to a mixture of 3,4,5-tris(hexadecyloxy)benzoic acid (842 mg, 1 mmol) and K_2CO_3 (279 mg, 2 mmol) in DMF (70 mL) under a nitrogen atmosphere. The reaction mixture was heated to reflux overnight. The reaction mixture was poured into deionized water and extracted with dichloromethane (3 times). The organic phase was washed with deionized water (3 times) and dried over anhydrous Na_2SO_4. Removal of the solvent under reduced pressure afforded the crude product, which was purified by column chromatography on silica gel using dichloromethane/hexane (2:1 v/v) as the eluent to give the desired product. Yield: 430 mg, 49 %. ^{1}H NMR (500 MHz, $CDCl_3$, 298 K, relative to Me_4Si): $\delta=0.88$ (t, $J=6.8$ Hz, 9H; CH_3), 1.26–1.30 (m, 72H; CH_2), 1.45–1.46 (m, 6H; CH_2), 1.72–1.81 (m, 6H; CH_2), 2.51 (t, $J=2.4$ Hz, 1H; $C{\equiv}CH$), 3.97–4.01 (m, 6H; OCH_2), 4.82 (d, $J=2.4$ Hz, 2H; $OCH_2C{\equiv}C$), 7.23 ppm (s, 2H; C_6H_2).

Synthesis of prop-2-ynylcholesteryl formate: A solution of cholesteryl chloroformate (449 mg, 1 mmol) in anhydrous dichloromethane (50 mL) was added to a solution of propargyl alcohol (112 mg, 2 mmol) and triethylamine (0.5 mL) in anhydrous dichloromethane (20 mL), under a nitrogen atmosphere, and the reaction mixture was stirred at room temperature overnight. The reaction solution was washed with an aqueous Na_2CO_3 solution (3 times) and dried over anhydrous Na_2SO_4. Removal of the solvent under reduced pressure afforded the desired product. Yield: 300 mg, 64 %. ^{1}H NMR (500 MHz, $CDCl_3$, 298 K, relative to Me_4Si): $\delta=0.67$ (s, 3H; cholesteryl proton), 0.85–1.60 (m, 33H; cholesteryl proton), 1.80–2.02 (m, 5H; cholesteryl proton), 2.37–2.40 (m, 2H; cholesteryl proton), 2.50 (t, $J=2.4$ Hz, 1H; $C{\equiv}CH$), 4.47–4.52 (m, 1H; OCH), 4.70 (d, $J=2.4$ Hz, 2H; $OCH_2C{\equiv}C$), 5.38 ppm (d, $J=5.1$ Hz, 1H; $HC{=}C$).

*Synthesis of **1***: The complex was synthesized according to a modification of a previously reported method for $[Pt(bpy)Cl_2]$ except 4-(1,3,3-trimethylspiroindolinenaphthoxazine-9′-oxymethyl)-4′-methyl-2,2′-bipyridine was used instead of 2,2′-bipyridine. A mixture of 4-(1,3,3-trimethylspiroindolinenaphthoxazine-9′-oxymethyl)-4′-methyl-2,2′-bipyridine (671 mg, 1.3 mmol) and $[Pt(dmso)_2Cl_2]$ (513 mg, 1.2 mmol) in dichloromethane (40 mL) was allowed to stir overnight. After removal of the solvents, diethyl ether (20 mL) was added. After filtration, the precipitate was washed with diethyl ether (10 mL) to yield the pure product. Yield: 920 mg, 91 %. ^{1}H NMR (500 MHz, $CDCl_3$, 298 K, relative to Me_4Si): $\delta=1.35$ (s, 6H; $C(CH_3)_2$), 2.57 (s, 3H; CH_3 on bpy), 2.76 (s, 3H; NCH_3), 5.42 (s, 2H; OCH_2 on bpy), 6.58 (d, $J=7.7$ Hz, 1H; indolinic proton at 7-position), 6.89–6.93 (m, 2H; indolinic proton at 5-position, naphthoxazinic proton at 5′-position), 7.09 (d, $J=7.7$ Hz, 1H; indolinic proton at 4-position), 7.18–7.24 (m, 2H; naphthoxazinic proton at 8′-position, indolinic proton at 6-position), 7.35 (d, $J=6.0$ Hz, 1H; bipyridine proton at 5′-position), 7.61–7.63 (m, 2H; naphthoxazinic proton at 6′-position, bipyridine at 5-position), 7.73 (s+d, $J=9.0$ Hz, 2H; naphthoxazinic proton at 2′,7′-position), 7.89 (s, 1H; bipyridine at 3′-position), 7.95 (d, $J=2.6$ Hz, 1H; naphthoxazinic proton at 10′-position), 8.17 (s, 1H; bipyridine at 3-position), 9.50 (d, $J=6.0$ Hz, 1H; bipyridine at 6′-position), 9.68 ppm (d, $J=6.1$ Hz, 1H; bipyridine at 6-position); positive FAB-MS: m/z: 793 $[M+H]^+$; elemental analysis calcd (%) for $C_{34}H_{30}Cl_2N_4O_2Pt$: C 51.52, H 3.82, N 7.07; found: C 51.78, H 3.91, N 7.20.

*Synthesis of **2***: The complex was synthesized according to a modification of a previously reported method for $[Pt(bpy)Cl_2]$ except that (4′-methyl-2,2′-bipyridin-4-yl)methyl-3,4,5-tris(hexadecyloxy)benzoate (192 mg, 0.19 mmol) was used instead of 2,2′-bipyridine. Yield: 230 mg, 95 %. ^{1}H NMR (500 MHz, $CDCl_3$, 298 K, relative to Me_4Si): $\delta=0.88$ (t, $J=6.8$ Hz, 9H; CH_3), 1.26–1.30 (m, 72H; CH_2), 1.46–1.55 (m, 6H; CH_2), 1.77–1.85 (m, 6H; CH_2), 2.54 (s, 3H; CH_3 on bpy), 4.00–4.06 (m, 6H; OCH_2), 5.45 (s, 2H; OCH_2 on bpy), 7.28 (d, $J=5.3$ Hz, bipyridine proton at 5′-position), 7.30 (s, 2H; C_6H_2), 7.48 (d, $J=5.2$ Hz, bipyridine proton at 5-position), 7.87 (s, bipyridine proton at 3′-position), 8.02 (s, bipyridine proton at 3-position), 9.36 (d, $J=5.3$ Hz, bipyridine proton at 6′-position), 9.52 ppm (d, $J=5.2$ Hz, bipyridine proton at 6-position); positive FAB-MS: m/z: 1293 $[M+H]^+$; elemental analysis calcd (%) for $C_{67}H_{112}Cl_2N_2O_5Pt{\cdot}CH_2Cl_2$: C 59.40, H 8.36, N 2.04; found: C 59.53, H 8.44, N 2.24.

*Synthesis of **3***: To a degassed solution of **2** (129 mg, 0.1 mmol) in dichloromethane (30 mL), diisopropylamine (5 mL), a catalytic amount of CuI (2 mg) and phenylacetylene (30.6 mg, 0.3 mmol) were added. The resulting solution was allowed to stir at room temperature for 24 h under a nitrogen atmosphere. After removal of solvents, the residue was purified by column chromatography on silica gel using dichloromethane/hexane (5:1 v/v) as the eluent to give the desired product. Yield: 99 mg, 70 %. ^{1}H NMR (500 MHz, CD_2Cl_2, 298 K, relative to CD_2Cl_2): $\delta=0.89$ (t, $J=6.8$ Hz, 9H; CH_3), 1.23–1.41 (m, 72H; CH_2), 1.44–1.53 (m, 6H; CH_2), 1.70–1.86 (m, 6H; CH_2), 2.91 (s, 3H; CH_3), 4.02–4.05 (m, 6H; OCH_2), 5.46 (s, 2H; $COOCH_2$), 7.16–7.21 (m, 2H; C_6H_5), 7.26–7.31 (m, 4H; C_6H_5), 7.33 (s, 2H; C_6H_2), 7.47–7.50 (m, 5H; bipyridine proton at 5′-position, C_6H_5), 7.66 (d, $J=5.5$ Hz, 1H; bipyridine proton at 5-position), 7.93 (s, 1H; bipyridine proton at 3′-position), 8.10 (s, 1H; bipyridine proton at 3-position), 9.61 (d, $J=5.5$ Hz, 1H; bipyridine proton at 6′-position), 9.61 ppm (d, $J=5.5$ Hz, 1H; bipyridine proton at 6-position); positive FAB-MS: m/z: 1425 $[M+H]^+$; elemental analysis calcd (%) for $C_{83}H_{122}N_2O_5Pt$: C 70.06, H 8.64, N 1.97; found: C 70.19, H 9.10, N 1.72.

*Synthesis of **4***: The procedure was similar to that for complex **3**, except $[Pt(bpy)Cl_2]$ (35 mg, 0.083 mmol) and prop-2-ynyl-3,4,5-tris(hexadecyloxy)benzoate (200 mg, 0.23 mmol) were used in place of **2** and phenylacetylene, respectively. Yield: 150 mg, 85 %. ^{1}H NMR (500 MHz, $CDCl_3$, 298 K, relative to Me_4Si): $\delta=0.88$ (t, $J=6.8$ Hz, 18H; CH_3), 1.19–1.29 (m, 144H; CH_2), 1.43–1.52 (m, 12H; CH_2), 1.72–1.83 (m, 12H; CH_2), 4.01–4.04 (m, 12H; OCH_2), 5.11 (s, 4H; $OCH_2C{\equiv}C$), 7.38–7.40 (m, 6H; C_6H_2, bipyridine proton at 4-position) 8.12 (t, $J=7.5$ Hz, 2H; bipyridine proton at 5-position), 8.25 (d, $J=7.5$ Hz, 2H; bipyridine proton at 3-position), 8.78 ppm (d, $J=6.3$ Hz, 2H; bipyridine proton at 6-position); positive FAB-MS: m/z: 2113 $[M+H]^+$; elemental analysis calcd (%) for $C_{126}H_{214}N_2O_{10}Pt{\cdot}2.5\,CHCl_3$: C 64.10, H 9.07, N 1.16; found: C 64.02, H 8.84, N 1.15.

*Synthesis of **5***: The procedure was similar to that for **3**, except **1** (100 mg, 0.13 mmol) was used in place of **2**. Yield: 60 mg, 54 %. ^{1}H NMR (500 MHz, $CDCl_3$, 298 K, relative to Me_4Si): $\delta=1.34$ (s, 6H; $C(CH_3)_2$), 2.51 (s, 3H; CH_3 on bpy), 2.75 (s, 3H; NCH_3), 5.39 (s, 2H; OCH_2 on bpy), 6.57 (d, $J=7.5$ Hz, 1H; indolinic proton at 7-position), 6.86–6.92 (m, 2H; indolinic proton at 5-position, naphthoxazinic proton at 5′-position), 7.07–7.23 (m, 9H; indolinic proton at 4,6-position, naphthoxazinic proton at 8′-position, C_6H_5), 7.30 (d, $J=5.4$ Hz, 1H; bipyridine proton at 5′-position), 7.50–7.52 (m, 4H; C_6H_5), 7.58–7.62 (m, 2H; naphthoxazinic proton at 6′-position, bipyridine proton at 5-position), 7.70 (s+d, $J=9.1$ Hz, 2H; naphthoxazinic proton at 2′,7′-position), 7.92–7.96 (m, 2H; naphthoxazinic proton at 10′-position, bipyridine proton at 3′-position), 8.24 (s, 1H; bipyridine proton at 3-position), 9.50 (d, $J=5.4$ Hz, 1H; bipyridine proton at 6′-position), 9.66 ppm (d, $J=5.5$ Hz, 1H; bipyridine proton at 6-position); positive FAB-MS: m/z: 924 $[M+H]^+$; elemental analysis calcd (%) for $C_{50}H_{40}N_4O_2Pt{\cdot}0.5\,CHCl_3$: C 61.66, H 4.15, N 5.70; found: C 61.68, H 4.47, N 5.79.

*Synthesis of **6***: The procedure was similar to that for **3**, except **1** (88.6 mg, 0.11 mmol) and 4-methoxyphenylacetylene (44 mg, 0.33 mmol) were used in place of **2** and phenylacetylene, respectively. Yield: 55 mg, 50 %. ^{1}H NMR (500 MHz, $CDCl_3$, 298 K, relative to Me_4Si): $\delta=1.34$ (s, 6H; $C(CH_3)_2$), 2.43 (s, 3H; CH_3 on bpy), 2.74 (s, 3H; NCH_3), 3.70 (s, 6H; OCH_3), 5.37 (s, 2H; OCH_2 on bpy), 6.57 (d, $J=7.8$ Hz, 1H; indolinic proton at 7-position), 6.71 (d, $J=8.3$ Hz, 4H; C_6H_4), 6.88–6.91 (m, 2H; indolinic proton at 5-position, naphthoxazinic proton at 5′-position), 7.07–7.11 (m, 2H; indolinic proton at 4-position, naphthoxazinic proton at 8′-position), 7.15 (d, $J=5.6$ Hz, 1H; bipyridine proton at 5′-position), 7.22 (dt, $J=1.0$, 7.7 Hz, 1H; indolinic proton at 6-position), 7.38–7.41 (m, 4H; C_6H_4), 7.48 (d, $J=5.7$ Hz, 1H; bipyridine proton at 5-position), 7.59 (d, $J=8.8$ Hz, 1H; naphthoxazinic proton at 6′-position), 7.66 (d, $J=8.9$ Hz, 1H; naphthoxazinic proton at 7′-position), 7.67 (s, 1H; naphthoxazinic proton at 2′-position), 7.87 (d, $J=2.4$ Hz, 1H; naphthoxazinic proton at 10′-position), 8.00 (s, 1H; bipyridine proton at 3′-position), 8.23

(s, 1H; bipyridine proton at 3-position), 9.28 (d, $J=5.6$ Hz, 1H; bipyridine proton at 6′-position), 9.42 ppm (d, $J=5.7$ Hz, 1H; bipyridine proton at 6-position); positive FAB-MS: m/z: 984 $[M+H]^+$; elemental analysis calcd (%) for $C_{52}H_{44}N_4O_4Pt{\cdot}1.5\,CHCl_3$: C 55.34, H 3.95, N 4.83; found: C 55.12, H 4.34, N 4.64.

*Synthesis of **7***: The procedure was similar to that for **3**, except **1** (100 mg, 0.13 mmol) and 4-ethynyl-α,α,α-trifluorotoluene (66.3 mg, 0.39 mmol) were used in place of **2** and phenylacetylene, respectively. Yield: 70 mg, 53%. ^{1}H NMR (500 MHz, $CDCl_3$, 298 K, relative to Me_4Si): $\delta=1.35$ (s, 6H; $C(CH_3)_2$), 2.55 (s, 3H; CH_3 on bpy), 2.76 (s, 3H; NCH_3), 5.42 (s, 2H; OCH_2 on bpy), 6.58 (d, $J=7.7$ Hz, 1H; indolinic proton at 7-position), 6.89–6.93 (m, 2H; indolinic proton at 5-position and naphthoxazinic proton at 5′-position), 7.09 (d, $J=7.2$ Hz, 1H; indolinic proton at 4-position), 7.18 (dd, $J=2.5$, 8.9 Hz, 1H; naphthoxazinic proton at 8′-position), 7.23 (t, $J=7.7$ Hz, 1H; indolinic proton at 6-position), 7.42 (d, $J=5.6$ Hz, 1H; bipyridine proton at 5′-position), 7.48 (d, $J=7.3$ Hz, 4H; C_6H_4), 7.58–7.60 (m, 4H; C_6H_4), 7.62 (d, $J=8.8$ Hz, 1H; naphthoxazinic proton at 6′-position), 7.68 (d, $J=5.7$ Hz, 1H; bipyridine proton at 5-position), 7.71 (s, 1H; naphthoxazinic proton at 2′-position), 7.73 (d, $J=8.9$ Hz, 1H; naphthoxazinic proton at 7′-position), 7.95–7.96 (m, 2H; naphthoxazinic proton at 10′-position and bipyridine proton at 3′-position), 8.26 (s, 1H; bipyridine proton at 3-position), 9.54 (d, $J=5.6$ Hz, 1H; bipyridine proton at 6′-position), 9.70 ppm (d, $J=5.7$ Hz, 1H; bipyridine proton at 6-position); positive FAB-MS: m/z: 1060 $[M+H]^+$; elemental analysis calcd (%) for $C_{52}H_{38}F_6N_4O_2Pt{\cdot}0.5\,CH_2Cl_2$: C 55.60, H 3.52, N 4.89; found: C 55.49, H 3.33, N 4.88.

*Synthesis of **8***: The procedure was similar to that for **3**, except **1** (110 mg, 0.14 mmol) and 3,4,5-tri(dodecyloxy)phenylacetylene (263 mg, 0.42 mmol) were used in place of **2** and phenylacetylene, respectively. Yield: 232 mg, 82%. ^{1}H NMR (500 MHz, $CDCl_3$, 298 K, relative to Me_4Si): $\delta=0.86$–0.89 (m, 18H; CH_3), 1.26–1.35 (m, 102H; CH_2, $C(CH_3)_2$), 1.41–1.46 (m, 12H; CH_2), 1.72–1.80 (m, 12H; CH_2), 2.53 (s, 3H; CH_3 on bpy), 2.75 (s, 3H; NCH_3), 3.91–3.96 (m, 12H; OCH_2), 5.39 (s, 2H; OCH_2 on bpy), 6.58 (d, $J=7.8$ Hz, 1H; indolinic proton at 7-position), 6.76 (s, 4H; C_6H_2), 6.90–6.92 (m, 2H; indolinic proton at 5-position, naphthoxazinic proton at 5′-position), 7.08 (d, $J=7.2$ Hz, 1H; indolinic proton at 4-position), 7.18 (dd, $J=2.5$, 8.8 Hz 1H; naphthoxazinic proton at 8′-position) 7.22–7.24 (m, 1H; indolinic proton at 6-position), 7.38 (d, $J=5.6$ Hz, 1H; bipyridine proton at 5′-position), 7.61–7.65 (m, 2H; naphthoxazinic proton at 6′-position, bipyridine proton at 5-position), 7.72 (s+d, $J=9.0$ Hz, 2H; naphthoxazinic proton at 2′,7 -position), 7.91–7.95 (m, 2H; naphthoxazinic proton at 10′-position, bipyridine proton at 3′-position), 8.21 (s, 1H; bipyridine proton at 3-position), 9.66 (d, $J=5.6$ Hz, 1H; bipyridine proton at 6′-position), 9.83 ppm (d, $J=5.7$ Hz, 1H; bipyridine proton at 6-position); positive FAB-MS: m/z: 2033 $[M+H]^+$; elemental analysis calcd (%) for $C_{122}H_{184}N_4O_8Pt{\cdot}0.5\,CH_2Cl_2$: C 71.00, H 9.00, N 2.70; found: C 71.37, H 8.78, N 2.70.

*Synthesis of **9***: The procedure was similar to that for **3**, except **1** (122 mg, 0.15 mmol) and 3,4,5-tri(hexadecyloxy)acetylene (369 mg, 0.45 mmol) were used in place of **2** and phenylacetylene, respectively. Yield: 320 mg, 88%. ^{1}H NMR (500 MHz, $CDCl_3$, 298 K, relative to Me_4Si): $\delta=0.80$–0.91 (m, 18H; CH_3), 1.27–1.35 (m, 150H; CH_2, $C(CH_3)_2$), 1.41–1.50 (m, 12H; CH_2), 1.74–1.79 (m, 12H; CH_2), 2.54 (s, 3H; CH_3 on bpy) , 2.76 (s, 3H; NCH_3), 3.93–3.97 (m, 12H; OCH_2), 5.43 (s, 2H; OCH_2 on bpy), 6.58 (d, $J=7.8$ Hz, 1H; indolinic proton at 7-position), 6.76 (s, 4H; C_6H_2), 6.91–6.93 (m, 2H; indolinic proton at 5-position, naphthoxazinic proton at 5′-position), 7.09 (d, $J=7.2$ Hz, 1H; indolinic proton at 4-position), 7.17 (dd, $J=2.6$ Hz, 8.9 Hz 1H; naphthoxazinic proton at 8′-position) 7.22–7.25 (m, 1H; indolinic proton at 6-position), 7.35 (d, $J=5.7$ Hz, 1H; bipyridine proton at 5′-position), 7.59–7.63 (m, 2H; naphthoxazinic proton at 6′-position, bipyridine proton at 5-position), 7.72 (s+d, $J=8.8$ Hz, 2H; naphthoxazinic proton at 2′,7′-position), 7.93–7.97 (m, 2H; naphthoxazinic proton at 10′-position, bipyridine proton at 3′-position), 8.25 (s, 1H; bipyridine proton at 3-position), 9.59 (d, $J=5.7$ Hz, 1H; bipyridine proton at 6′-position), 9.83 ppm (d, $J=5.7$ Hz, 1H; bipyridine proton at 6-position); positive FAB-MS: m/z: 2366 $[M+H]^+$; elemental analysis calcd (%) for $C_{146}H_{232}N_4O_8Pt{\cdot}0.5\,CH_2Cl_2$: C 73.04, H 9.75, N 2.32; found: C 72.90, H 9.43, N 2.25.

*Synthesis of **10***: The procedure was similar to that for **3**, except **1** (158 mg, 0.20 mmol) and prop-2-ynylcholesteryl formate (281 mg, 0.60 mmol) were used in place of **2** and phenylacetylene, respectively. Yield: 245 mg, 74%. ^{1}H NMR (500 MHz, $CDCl_3$, 298 K, relative to Me_4Si): $\delta=0.66$ (s, 3H; 3H; cholesteryl proton), 0.86–1.64 (m, 72H; cholesteryl proton and -$(CH_3)_2$), 1.79–2.03 (m, 10H; cholesteryl proton), 2.35–2.37 (m, 4H; cholesteryl proton), 2.57 (s, 3H; CH_3 on bpy), 2.74 (s, 3H; NCH_3), 4.45–4.51 (m, 2H; OCH on cholesteryl proton), 5.11 (s, 4H; $OCH_2C{\equiv}C$), 5.35 (s, 2H; CH=C on cholesteryl), 5.50 (s, 2H; OCH_2 on bpy), 6.56 (d, $J=7.8$ Hz, 1H; indolinic proton at 7-position), 6.88–6.91 (m, 2H; indolinic proton at 5-position and naphthoxazinic proton at 5′-position), 7.07 (d, $J=6.6$ Hz, 1H; indolinic proton at 4-position), 7.15 (dd, $J=2.6$, 8.9 Hz 1H; naphthoxazinic proton at 8′-position) 7.20–7.23 (m, 2H; indolinic proton at 6-position and bipyridine proton at 5′-position), 7.51 (d, $J=5.6$ Hz, 1H; bipyridine proton at 5-position), 7.60 (d, $J=8.9$ Hz, 1H; naphthoxazinic proton at 6′-position), 7.70 (s+d, $J=8.7$ Hz, 2H; naphthoxazinic proton at 2′,7′-position), 7.79 (d, $J=2.3$ Hz, 1H; naphthoxazinic proton at 10′-position), 8.01 (s, 1H; bipyridine proton at 3′-position), 8.25 (s, 1H; bipyridine proton at 3-position), 9.23 (d, $J=5.6$ Hz, 1H; bipyridine proton at 6′-position), 9.40 ppm (d, $J=5.6$ Hz, 1H; bipyridine proton at 6-position); positive FAB-MS: m/z: 1657 $[M+H]^+$; elemental analysis calcd (%) for $C_{96}H_{124}N_4O_8Pt$: C 69.58, H 7.54, N 3.38; found: C 69.63, H 7.84, N 3.12.

Physical measurements and instrumentation: ^{1}H NMR spectra were recorded on a Bruker DRX 500 (500 MHz) spectrometer at 298 K. Chemical shifts (δ, ppm) were reported relative to tetramethylsilane (Me_4Si). Positive ion FAB mass spectra were recorded on a Finnigan MAT95 mass spectrometer. Elemental analyses of the complexes were performed on a Flash EA 1112 elemental analyzer at Jilin University.

Cyclic voltammetric measurements were performed by using a CH Instruments, Inc. model CHI 660C electrochemical analyzer. Electrochemical measurements were performed in a dichloromethane solution with 0.1 M $n\mathrm{Bu_4NPF_6}$ (TBAH) as supporting electrolyte at room temperature. The reference electrode was an $Ag/AgNO_3$ (0.1 mol dm^{-3} in acetonitrile) electrode and the working electrode was a glassy carbon electrode (CH Instruments, Inc.) with a platinum wire as the counter electrode. The working electrode surface was first polished with a 1 μm alumina slurry (Linde) on a microcloth (Buehler Co.) and then with a 0.3 μm alumina slurry. It was then rinsed with ultra-pure deionized water and sonicated in a beaker containing ultra-pure water for five minutes. The polishing and sonicating steps were repeated twice and then the working electrode was finally rinsed under a stream of ultra-pure deionized water. The ferrocenium/ferrocene couple ($FeCp_2^{+/0}$) was used as the internal reference.[26] All solutions for electrochemical studies were deaerated with pre-purified argon gas prior to measurements.

Electronic absorption spectra were obtained using a Varian Cary 50 UV/Vis spectrophotometer. Steady state excitation and emission spectra at room temperature and at 77 K and emission lifetimes were recorded on a Horiba–Jobin–Yvon Fluorolog-3 fluorescence spectrofluorometer equipped with a R928P PMT detector and a time-correlated single-photon counting (TCSPC) system, respectively. For the lifetime measurements, the excitation source was a 370 nm output of a nanoLED pulsed laser diode. Luminescence decay signals were detected by a TBX-04 photomultiplier tube module and analyzed by using IBH lifetime analysis for exponential fits. Solid-state photophysical studies were carried out with solid samples contained in a quartz tubes inside a quartz-walled Dewar flask. Measurements of the glass state in ethanol/methanol/dichloromethane = 4:1:1 or a solid-state sample at 77 K were similarly conducted with liquid nitrogen filled in the optical Dewar flask. All of the solutions for the photophysical studies were degassed on a high-vacuum line in a two-compartment cell consisting of a 10 mL Pyrex bulb and a 1 cm path length quartz cuvette that was sealed from the atmosphere by a Bibby Rotaflo HP6 Teflon stopper. The solutions were rigorously degassed with at least four successive freeze-pump-thaw cycles. Luminescence quantum yields were measured by the optical dilute method reported by Demas and Crosby.[27] A degassed solution of $[Ru(bpy)_3]Cl_2$ in acetonitrile ($\phi = 0.062$, excitation wavelength at 436 nm) was used as the reference.[28]

The kinetics for the bleaching reaction were determined by measurement of the UV/Vis spectral changes at various temperatures with the use of a Varian Cary 50 UV/Vis spectrophotometer, with the temperature controlled by a single cell Peltier thermostat. Photoirradiation was carried out using monochromatic light at 405 nm. The thermal bleaching reaction of spironaphthoxazines is known to follow first-order kinetics at various temperatures. The first-order rate constants were obtained by taking the negative value of the slope of a linear least-squares fit of $\ln[(A-A_\infty)/(A_0-A_\infty)]$ against time according to Equation (1), in which A, A_0, and A_∞ are the absorbance at the absorption wavelength maximum of the open form at times t, 0, and infinity, respectively, and k is the rate constant of the reaction. The kinetic parameters were obtained by a linear least-squares fit of $\ln(k/T)$ against $1/T$ according to the linear expression of the Eyring equation [Eq. (2)] and $\ln k$ against $1/T$ according to the Arrhenius equation [Eq. (3)], in which $\Delta H^{\ddagger}$ and $\Delta S^{\ddagger}$ are the changes in enthalpy of activation and entropy of activation, respectively, E_a is the activation energy, T is the temperature, and k_B, R, h, and A are the Boltzmann constant, the universal gas constant, the Planck constant, and the frequency factor, respectively.

$$\ln\left(\frac{A-A_\infty}{A_0-A_\infty}\right) = -kt \tag{1}$$

$$\ln\left(\frac{k}{T}\right) = -\left(\frac{\Delta H^{\ddagger}}{R}\right)\left(\frac{1}{T}\right) + \ln\left(\frac{k_B}{h}\right) + \frac{\Delta S^{\ddagger}}{R)} \tag{2}$$

$$\ln(k) = -\frac{E_a}{RT} + \ln A \tag{3}$$

For the spectroscopic and luminescence studies of metallogels, the instruments used for the variable-temperature electronic absorption and emission measurements were the same as those described above. A single cell Peltier thermostat was used to control the working temperature in the range of 10 to 70 °C. The gel samples were measured in 1 mm or 0.1 mm path-length quartz cuvettes and 4 mm-path-length quartz cuvettes for electronic absorption and emission experiments, respectively.

Thermogravimetric analyses (TGA) were conducted on a Perkin–Elmer Diamond TG/DTA instrument with a heating rate of $10\,K\,min^{-1}$ under flowing air. Differential scanning calorimetry (DSC) measurements were performed on a Netzsch DSC 204. The scanning rate was $5\,K\,min^{-1}$. The samples were sealed in aluminum capsules in air, and the holder atmosphere was anhydrous nitrogen. Variable-temperature X-ray diffraction (XRD) experiments were carried out on a Rigaku X-ray diffractometer (D/max 2500 V, using Cu $K\alpha_1$ radiation with a wavelength of 1.5 Å) with a PTC-20 A temperature controller. Variable-temperature infrared (IR) spectra were performed on a Bruker IFS66 V Fourier transform infrared spectrometer, equipped with a DTGS detector with a resolution of $4\,cm^{-1}$, from pressed KBr pellets. The heating rate was $5\,K\,min^{-1}$ over the temperature range of 30–180 °C.

Scanning electron microscopy measurements were performed on a JEOL JSM-6700F field-emission scanning electron microscope. The SEM sample was prepared by dropping dilute gels onto a silicon wafer. Slow evaporation of solvents in air for 10 min led to xerogels.

Gelation test: The gelator and the solvent were placed in a screw-capped sample vial and the mixture was heated until the solid had dissolved. The sample vial was cooled, and was then left for 1 h at room temperature. The state of the materials was evaluated by the "stable-to-inversion of a test tube" method. Using **10** as an example, the sample (1.20 mg) was dissolved in a minimum amount of dichloromethane in a vial and 0.3 mL of dodecane were placed into the sample vial and the mixture was heated to 80 °C for about 1 h until all of the dichloromethane had evaporated. The sample vial was left for 1 h undisturbed. A stable organogel was formed, and the gelation was evaluated by the "stable-to-inversion of a test tube" method.

Acknowledgements

V.W.-W.Y. acknowledges support from The University of Hong Kong under the Distinguished Research Achievement Award Scheme. We also acknowledge support from the State Key Laboratory of Supramolecular Structure and Materials, Jilin University and The University of Hong Kong. This work has been supported by the University Grants Committee Areas of Excellence Scheme (AoE/P-03/08) and a General Research Fund (GRF) grant from the Research Grants Council of Hong Kong Special Administrative Region, China (HKU 7060/09P). A.Y.-Y.T. acknowledges the receipt of a University Postdoctoral Fellowship from The University of Hong Kong.

[1] a) V. M. Miskowski, V. H. Houlding, C. M. Che, Y. Wang, *Inorg. Chem.* **1993**, *32*, 2518; b) B. C. Tzeng, W. F. Fu, C. M. Che, H. Y. Chao, K. K. Cheung, S. M. Peng, *J. Chem. Soc. Dalton Trans.* **1999**, 1017; c) V. M. Miskowski, V. H. Houlding, *Inorg. Chem.* **1991**, *30*, 4446; d) V. W. W. Yam, R. P. L. Tang, K. M. C. Wong, K. K. Cheung, *Organometallics* **2001**, *20*, 4476; e) V. W. W. Yam, K. M. C. Wong, N. Zhu, *J. Am. Chem. Soc.* **2002**, *124*, 6506; f) V. W. W. Yam, K. H. Y. Chan, K. M. C. Wong, N. Zhu, *Chem. Eur. J.* **2005**, *11*, 4535; g) K. M. C. Wong, W. S. Tang, B. W. K. Chu, N. Zhu, V. W. W. Yam, *Organometallics* **2004**, *23*, 3459; h) H. K. Yip, L. K. Cheng, K. K. Cheung, C. M. Che, *J. Chem. Soc. Dalton Trans.* **1993**, 2933; i) J. A. Bailey, M. G. Hill, R. E. Marsh, V. M. Miskowski, W. P. Schaefer, H. B. Gray, *Inorg. Chem.* **1995**, *34*, 4591.

[2] a) V. M. Miskowski, V. H. Houlding, *Inorg. Chem.* **1989**, *28*, 1529; b) E. J. L. McInnes, R. D. Farley, S. A. Macgregor, K. J. Taylor, L. J. Yellowlees, C. C. Rowlands, *J. Chem. Soc. Faraday Trans.* **1998**, *94*, 2985; c) B. C. Tzeng, S. C. Chan, M. C. W. Chan, C. M. Che, K. K. Cheung, S. M. Peng, *Inorg. Chem.* **2001**, *40*, 6699; d) K. W. Lee, C. C. Ko, K. M. C. Wong, N. Zhu, V. W. W. Yam, *Organometallics* **2007**, *26*, 12; e) D. Pucci, G. Barberio, A. Crispini, O. Francescangeli, M. Ghedini, M. La Deda, *Eur. J. Inorg. Chem.* **2003**, 3649.

[3] a) W. B. Connick, D. Geiger, R. Eisenberg, *Inorg. Chem.* **1999**, *38*, 3264; b) B. H. Xia, C. M. Che, D. L. Phillips, K. H. Leung, K. K. Cheung, *Inorg. Chem.* **2002**, *41*, 3866; c) M. Kato, C. Kosuge, K. Morii, J. S. Ahn, H. Kitagawa, T. Mitani, M. Matsushita, T. Kato, S. Yano, M. Kimura, *Inorg. Chem.* **1999**, *38*, 1638.

[4] C. W. Chan, L. K. Cheng, C. M. Che, *Coord. Chem. Rev.* **1994**, *132*, 87.

[5] a) M. Hissler, W. B. Connick, D. K. Geiger, J. E. McGarrah, D. Lipa, R. J. Lachicotte, R. Eisenberg, *Inorg. Chem.* **2000**, *39*, 447; b) C. Ed. Whittle, J. A. Weinstein, M. W. George, K. S. Schanze, *Inorg. Chem.* **2001**, *40*, 4053; c) F. Hua, S. Kinayyigit, J. R. Cable, F. N. Castellano, *Inorg. Chem.* **2006**, *45*, 4304; d) F. Hua, S. Kinayyigit, A. A. Rachford, E. A. Shikhova, S. Goeb, J. R. Cable, C. J. Adams, K. Kirschbaum, A. A. Pinkerton, F. N. Castellano, *Inorg. Chem.* **2007**, *46*, 8771; e) S. Chakraborty, T. J. Wadas, H. Hester, R. Schmehl, R. Eisenberg, *Inorg. Chem.* **2005**, *44*, 6865.

[6] a) R. J. Hovey, C. H. Fuchsman, N. Y. C. Chu, P. G. Piusz (American Optical Co., Southbridge, MA), U.S. Patent, 4215010, **1980**; b) H. Ono, C. Osada, U.S. Patent, 3562172, **1971**; c) A. Kellmann, F. Tfibel, R. Dubest, P. Levoir, *J. Photochem. Photobiol. A* **1989**, *49*, 63; d) A. K. Chibisov, H. Görner, *J. Phys. Chem. A* **1999**, *103*, 5211; e) V. W. W. Yam, S. H. F. Chong, C. C. Ko, K. K. Cheung, *Organometallics* **2000**, *19*, 5092; f) A. V. Metelitsa, J. C. Micheau, N. A. Voloshin, E. N. Voloshina, V. I. Minkin, *J. Phys. Chem. A* **2001**, *105*, 8417; g) M. Querol, B. Bozic, N. Salluce, P. Belser, *Polyhedron* **2003**, *22*, 655; h) C. C. Ko, L. Wu, K. M. C. Wong, N. Zhu, V. W. W. Yam, *Chem. Eur. J.* **2004**, *10*, 766; i) R. T. F. Jukes, B. Bozic, F. Hartl, P. Belser, L. De Cola, *Inorg. Chem.* **2006**, *45*, 8326; j) Z. Bao, K. Y. Ng, V. W. W. Yam, C. C. Ko, N. Zhu, L. Wu, *Inorg. Chem.* **2008**, *47*, 8912; k) Y. Hirshberg, *Bull. Res. Council Isr.* **1956**, *5A*, 188; l) Y. Hirshberg, *J. Am. Chem. Soc.* **1956**, *78*, 2304; m) A. S. Dvornikov, P. M. Rentzepis, *Mol. Cryst. Liq. Cryst. Sci. Technol. Sect. A* **1994**, *246*, 379; n) G. Berkovic, V. Krongauz, V. Weiss, *Chem. Rev.* **2000**, *100*, 1741; o) R. T. F. Jukes, B. Bozic, P. Belser, L. De Cola, F. Hartl,

Inorg. Chem. **2009**, *48*, 1711; p) V. W. W. Yam, C. C. Ko, N. Zhu, *J. Am. Chem. Soc.* **2004**, *126*, 12734; q) P. H. M. Lee, C. C. Ko, N. Zhu, V. W. W. Yam, *J. Am. Chem. Soc.* **2007**, *129*, 6058; r) V. W. W. Yam, J. K. W. Lee, C. C. Ko, N. Zhu, *J. Am. Chem. Soc.* **2009**, *131*, 912; s) C. C. Ko, V. W. W. Yam, *J. Mater. Chem.* **2010**, *20*, 2063.

[7] a) Y. Lin, R. G. Weiss, *Macromolecules* **1987**, *20*, 414; b) I. Furmant, R. G. Weiss, *Langmuir* **1993**, *9*, 2084; c) R. Mukkamala, R. G. Weiss, *Langmuir* **1996**, *12*, 1474; d) P. Terech, R. G. Weiss, *Chem. Rev.* **1997**, *97*, 3133; e) D. J. Abdallah, R. G. Weiss, *Adv. Mater.* **2000**, *12*, 1237, f) L. Lu, T. M. Cocker, R. E. Bachman, R. G. Weiss, *Langmuir* **2000**, *16*, 20.

[8] a) K. Murata, M. Aoki, T. Suzuki, T. Harada, H. Kawabata, T. Komri, F. Olrseto, K. Ueda, S. Shinkai, *J. Am. Chem. Soc.* **1994**, *116*, 6664; b) K. Sugiyasu, N. Fujita, S. Shinkai, *Angew. Chem.* **2004**, *116*, 1249; *Angew. Chem. Int. Ed.* **2004**, *43*, 1229; c) T. Kitahara, M. Shirakawa, S. Kawano, U. Beginn, N. Fujita, S. Shinkai, *J. Am. Chem. Soc.* **2005**, *127*, 14980; d) N. Fujita, Y. Sakamoto, M. Shirakawa, M. Ojima, A. Fujii, M. Ozaki, S. Shinkai, *J. Am. Chem. Soc.* **2007**, *129*, 4134.

[9] F. Camerel, L. Bonardi, G. Ulrich, L. Charbonnière, B. Donnio, C. Bourgogne, D. Guillon, P. Retailleau, R. Ziessel, *Chem. Mater.* **2006**, *18*, 5009.

[10] a) H. Kobayashi, A. Friggeri, K. Koumoto, M. Amaike, S. Shinkai, D. N. Reinhoudt, *Org. Lett.* **2002**, *4*, 1423; b) H. Kobayashi, K. Koumoto, J. H. Jung, S. Shinkai, *J. Chem. Soc. Perkin Trans. 2* **2002**, 1930; c) S. van der Laan, B. L. Feringa, R. M. Kellogg, J. H. van Esch, *Langmuir* **2002**, *18*, 7136; d) J. H. Jung, S. Shinkai, T. Shimizu, *Nano Lett.* **2002**, *2*, 17; e) J. Mamiya, K. Kanie, T Hiyama, T. Ikeda, T. Kato, *Chem. Commun.* **2002**, 1870; f) M. Moriyama, N. Mizoshita, T. Yokota, K. Kishimoto, T. Kato, *Adv. Mater.* **2003**, *15*, 1335.

[11] J. J. D. de Jong, J. N. Lucas, R. M. Kellogg, J. H. van Esch, B. L. Feringa, *Science* **2004**, *304*, 278.

[12] a) S. Wang, W. Shen, Y. Feng, H. Tian, *Chem. Commun.* **2006**, 1497; b) H. Tian, S. Wang, *Chem. Commun.* **2007**, 781.

[13] H. Hachisako, I. Ihara, T. Kamiya, C. Hirayama, K. Yamada, *Chem. Commun.* **1997**, 19.

[14] a) S. A. Ahmed, X. Sallenave, F. Fages, G. M. Gundert, W. M. Müller, U. Müller, F. Vögtle, J. L. Pozzo, *Langmuir* **2002**, *18*, 7096; b) A. R. Katritzky, R. Sakhuja, S. K. Khelashvili, *J. Org. Chem.* **2009**, *74*, 3062.

[15] Y. Li, K. M. C. Wong, A. Y. Y. Tam, L. Wu, V. W. W. Yam, *Chem. Eur. J.* **2010**, *16*, 8690.

[16] F. Fages, *Angew. Chem.* **2006**, *118*, 1710; *Angew. Chem. Int. Ed.* **2006**, *45*, 1680.

[17] a) A. Kishimura, T. Yamashita, T. Aida, *J. Am. Chem. Soc.* **2005**, *127*, 179; b) S. Kawano, N. Fujita, S. Shinkai, *J. Am. Chem. Soc.* **2004**, *126*, 8592; c) M. Shirakawa, N. Fujita, T. Tani, K. Kaneko, S. Shinkai, *Chem. Commun.* **2005**, 4149; d) F. Camerel, L. Bonardi, M. Schmutz, R. Ziessel, *J. Am. Chem. Soc.* **2006**, *128*, 4548; e) T. Naota, H. Koori, *J. Am. Chem. Soc.* **2005**, *127*, 9324, f) W. Weng, J. B. Beck, A. M. Jamieson, S. J. Rowan, *J. Am. Chem. Soc.* **2006**, *128*, 11663; g) T. Tu, W. Aseenmacher, H. Peterlik, R. Weisbarth, M. Nieger, K. H. Dötz, *Angew. Chem.* **2007**, *119*, 6486; *Angew. Chem. Int. Ed.* **2007**, *46*, 6368; h) T. Cardolaccia, Y. Li, K. S. Schanze, *J. Am. Chem. Soc.* **2008**, *130*, 2535; i) S. T. Lam, G. Wang, V. W. W. Yam, *Organometallics* **2008**, *27*, 4545; j) M. Shirakawa, N. Fujita, T. Tani, K. Kaneko, M. Ojima, A. Fujii, M. Ozaki, S. Shinkai, *Chem. Eur. J.* **2007**, *13*, 4155.

[18] a) A. Y. Y. Tam, K. M. C. Wong, G. X. Wang, V. W. W. Yam, *Chem. Commun.* **2007**, 2028; b) A. Y. Y. Tam, K. M. C. Wong, N. Y. Zhu, G. X. Wang, V. W. W. Yam, *Langmuir* **2009**, *25*, 8685; c) F. Camerel, R. Ziessel, B. Donnio, C. Bourgogne, D. Guillon, M. Schmutz, C. Iacovita, J. P. Bucher, *Angew. Chem.* **2007**, *119*, 2713; *Angew. Chem. Int. Ed.* **2007**, *46*, 2659; d) A. Y. Y. Tam, K. M. C. Wong, V. W. W. Yam, *J. Am. Chem. Soc.* **2009**, *131*, 6253; e) A. Y. Y. Tam, K. M. C. Wong, V. W. W. Yam, *Chem. Eur. J.* **2009**, *15*, 4775.

[19] D. W. Bruce, J. W. Goodby, J. R. Sambles, H. J. Coles, *Phil. Trans. R. Soc. A* **2006**, *364*, 2567.

[20] D. Pucci, G. Barberio, A. Bellusci, A. Crispini, B. Donnio, L. Giorgini, M. Ghedini, M. La Deda, E. I. Szerb, *Chem. Eur. J.* **2006**, *12*, 6738.

[21] R. Bayón, S. Coco, P. Espinet, *Chem. Eur. J.* **2005**, *11*, 1079.

[22] a) K. Venkatesan, P. H. J. Kouwer, S. Yagi, P. Müller, T. M. Swager, *J. Mater. Chem.* **2008**, *18*, 400; b) C. Damm, G. Israel, T. Hegmann, C. Tschierske, *J. Mater. Chem.* **2006**, *16*, 1808; c) A. Santoro, A. C. Whitwood, J. A. G. Williams, V. N. Kozhevnikov, D. W. Bruce, *Chem. Mater.* **2009**, *21*, 3871.

[23] a) M. Ghedini, D. Pucci, A. Crispini, A. Bellusci, M. La Deda, I. Aiello, T. Pugliese, *Inorg. Chem. Commun.* **2007**, *10*, 243; b) G. Barberio, A. Bellusci, A. Crispini, M. Ghedini, A. Golemme, P. Prus, D. Pucci, *Eur. J. Inorg. Chem.* **2005**, 181.

[24] F. Gao, L. Yang, L. Yang, H. Li, S. Zhang, *J. Fluoresc.* **2010**, *20*, 353.

[25] Most fluid smectic liquid crystals, with the exception of amphiphilic molecules, mesogenic sugars and other related species, generally only showed the first-order diffraction peak; selected examples have been reported in a) I. Dierking, *Textures of Liquid Crystals*, Wiley-VCH, Weinheim, **2003**, p. 9–10; b) I. Dierking, *Textures of Liquid Crystals*, Wiley-VCH, Weinheim, **2003**, p. 206; c) N. Tamaoki, Y. Aoki, M. Moriyama, M. Kidowak, *Chem. Mater.* **2003**, *15*, 719; d) L. Cui, Y. Zhao, *Chem. Mater.* **2004**, *16*, 2076.

[26] N. G. Connelly, W. E. Geiger, *Chem. Rev.* **1996**, *96*, 877.

[27] G. A. Crosby, J. N. Demas, *J. Phys. Chem.* **1971**, *75*, 991.

[28] L. Wallace, D. P. Rillema, *Inorg. Chem.* **1993**, *32*, 3836.

Received: December 28, 2010
Revised: April 2, 2011